Neuroradiology (2020) 62:705–713
https://doi.org/10.1007/s00234-020-02386-z

PAEDIATRIC NEURORADIOLOGY

Role of susceptibility-weighted imaging and intratumoral susceptibility signals in grading and differentiating pediatric brain tumors at 1.5 T: a preliminary study

Simona Gaudino[1] · Giammaria Marziali[1,2] · Giovanna Pezzullo[3] · Pamela Guadalupi[1,2] · Carolina Giordano[1,2] · Amato Infante[4] · Massimo Benenati[1,2] · Antonia Ramaglia[1,2] · Luca Massimi[5,6] · Marco Gessi[7] · Paolo Frassanito[5] · Massimo Caldarelli[5,6] · Cesare Colosimo[1,2]

Received: 1 October 2019 / Accepted: 25 February 2020 / Published online: 6 March 2020

Abstract

Purpose Susceptibility-weighted imaging (SWI) is useful for glioma grading and discriminating between brain tumor categories in adults, but its diagnostic value for pediatric brain tumors is unclear. Here we evaluated the usefulness of SWI for pediatric tumor grading and differentiation by assessing intratumoral susceptibility signal intensity (ITSS).

Methods We retrospectively enrolled 96 children with histopathologically diagnosed brain tumors, who underwent routine brain MRI exam with SWI (1.5 T scanner). Each tumor was assigned an ITSS score by a radiology resident and an experienced neuroradiologist, and subsequently by consensus. Statistical analyses were performed to differentiate between low-grade (LG) and high-grade (HG) tumors, histological categories, and tumor locations. Inter-reader agreement was assessed using Cohen's kappa (κ).

Results The interobserver agreement was 0.844 (0.953 between first reader and consensus, and 0.890 between second reader and consensus). Among all tumors, we found a statistically significant difference between LG and HG for ITSS scores of 0 and 2 ($p = 0.002$). This correlation was weaker among astrocytomas alone, and became significant when considering only off-midline astrocytomas ($p = 0.05$). Scores of 0 and 2 were a strong discriminating factor ($p = 0.001$) for astrocytomas (score 0) and for embryonal, choroid plexus, germ-cell, pineal, and ependymoma tumors (score 2). No medulloblastoma showed a score of 0.

Conclusions Our preliminary ITTS results in pediatric brain tumors somewhat differed from those obtained in adult populations. These findings highlight the potential valuable role of ITSS for tumor grading and discriminating between some tumor categories in the pediatric population.

Keywords Pediatric · Swi · Tumor · ITSS · Brain

✉ Simona Gaudino
simona.gaudino@policlinicogemelli.it

Giammaria Marziali
giammaria.marziali@gmail.com

Giovanna Pezzullo
gio_pezzullo@libero.it

Pamela Guadalupi
pamela.guadalupi@gmail.com

Carolina Giordano
carolinagiordano91@gmail.com

Amato Infante
amatoinfante@gmail.com

Massimo Benenati
maxbene3@gmail.com

Antonia Ramaglia
ramaglia88@gmail.com

Luca Massimi
lmassimi@email.it

Marco Gessi
marco.gessi@policlinicogemelli.it

Paolo Frassanito
paolo.frassanito@policlinicogemelli.it

Massimo Caldarelli
massimo.caldarelli@policlinicogemelli.it

Cesare Colosimo
cesare.colosimo@policlinicogemelli.it

Extended author information available on the last page of the article

Introduction

Central nervous system (CNS) neoplasms are the most frequent solid tumors in children, constituting a primary cause of mortality. Until recently, pediatric brain tumors were diagnosed and classified exclusively based on histologic criteria, and treatments were empirically chosen. The current five-year survival rate is 73.6% among children under 19 years of age, with variation according to the tumor's unique histologic and molecular characteristics [1]. Recent research has greatly enhanced our understanding of the diverse biology of pediatric brain tumors, including their molecular and genetic underpinnings leading to improved diagnostic accuracy and risk stratification, and the development of novel biomarkers and molecular targeted therapies [2].

Magnetic resonance imaging (MRI) plays several key roles in the management of pediatric brain tumors, including diagnosis, prognosis, and treatment response assessment. Imaging can provide morphological data about the lesion, as well as functional information regarding its cellularity, metabolism, permeability, neoangiogenesis, and cell turnover. Some advanced sequences, such as DWI, PWI, and MRS, are now included in the clinical study protocols for adult brain tumors [3]. However, their validation in the pediatric context remains controversial, due to both the poor technical reproducibility of the sequences used in adults, and the histological and genetic heterogeneity of tumors found in small patients. Susceptibility-weighted imaging (SWI) is among the most recent non-morphological magnetic resonance sequences [4–7], and has demonstrated good diagnostic performance as an index of glioma grading and in the differential diagnosis between tumor histotypes, as glioblastoma and primary cerebral lymphoma [4–9].

SWI is sensitive to blood products with magnetic susceptibility effect, as intratumoral accumulation of hemosiderin (extravascular blood degradation products) and increase in the concentration of deoxyhemoglobin in the venous blood, due to altered permeability of tumor, neoangiogenesis, and the increased cerebral blood volume.

Intratumoral susceptibility signals (ITSS) are defined as clearly hypointense spots on SWI, having linear or point morphology, and with or without conglomeration. Qualitative and quantitative/semi-quantitative evaluation of ITSS enables the definition of an index of tumor aggressiveness in the adult population [9–11]. With regard to pediatric brain tumors, the diagnostic capabilities of SWI are scarcely reported in the literature, and the ITSS score has not yet been applied [12].

Clinical evidence supporting the usefulness of these sequences for brain tumor evaluation remains controversial; however, even minimal support to conventional MRI findings is a desirable goal. In the present study, we aimed to investigate the potential role of the ITSS score in the evaluation of pediatric brain tumors.

Methods

Patient population

We retrospectively evaluated all consecutive pediatric patients with primary brain tumors who underwent MRI examination at our institution between February 2013 and April 2019. The inclusion criteria were histopathologic diagnosis of primary brain tumor according to the World Health Organization classification of tumors of the central nervous system 2016; no previous surgery, radiotherapy, or chemotherapy; and preoperative MRI examination including SWI sequence. Informed consent and Institutional Review Board approval (from IRB of Catholic University of Rome) were obtained.

This study enrolled a total of 96 patients with brain tumors; age at diagnosis ranged from1 to 16 years, (median 9.6 years, standard deviation 5.0 years). Of the 96 included tumors, 46 were astrocytomas—including 27 pilocytic astrocytomas (PA), 3 low-grade astrocytomas, 13 diffuse midline glioma H3K27M-m tumors, and three GBM. Twenty-four included tumors were neuronal and mixed glioneuronal tumors—including 3 DNT, 12 gangliogliomas, 3 central neurocytomas, and 6 NOS (not otherwise specified) glioneuronal tumors. Ten included tumors were embryonal lesions—including 7 medulloblastomas, 1 neuroblastoma, and 2 embryonal tumors with multilayered rosettes (ETMR). The remaining 16 tumors were categorized as "other"—including 6 germ cell tumors, 4 choroid plexus tumors, 4 ependymomas, and 2 pineal region tumors. Fifty-seven of 96 lesions were of low grade (LG), 39/96 of high grade (HG). Regarding tumor location, 45 were supratentorial and 51 infratentorial, and 55 involved the midline while 41 were off-midline (Table 1).

Image acquisition

All examinations were performed using a 1.5 T MR system (Ingenia - Philips, Best, The Netherlands) with an eight-channel head coil. All patients underwent T1-weighted imaging (T1WI), T2WI, fluid-attenuated inversion recovery, DWI, SWI, and contrast-enhanced T1WI. Imaging parameters for SWI were as follows: TR/TE, 26/50 msec; FA, 20°; slice thickness, 2 mm; slice gap; voxel size 0.9 × 1.06 × 2 mm, 130 slices; acquisition time: 3′ and 55″.

Data analysis

All images were independently analyzed by two readers—one neuroradiologist with over 10 years of experience (SG) and a radiologist resident with 4 years of experience (GP)—who were double blinded to the histopathological results and to each other's scores. Both readers first evaluated the extent of the lesion using FLAIR sequences. Corrected-phase images and magnitude images were obtained using the SWI post-

Table 1 Summary table of the patient population

Histotype	Number Of Patients	Subgroup	Grading: "low grade"	Grading: "high grade"	Localization: Infratentorial	Localization: Supratentorial	Localization: Midline	Localization: Off-Midline
Astrocytomas	46	0	30	16	34	12	28	18
Pilocytic Astrocytoma	27		27	0	18	9	12	15
LG Astrocytoma	3		3	0	2	1	2	1
Diffuse Midline H3k27m	13		0	13	13	0	13	0
GBM	3		0	3	1	2	1	2
Ependymomas	4	1	0	4	3	1	3	1
Choroid Plexuses Tumors	4	2	3	1	4	0	4	0
Carcinoma Choroid Plexus	1		0	1	1	0	1	0
Papilloma Choroid Plexus	3		3	0	3	0	**3**	**0**
Germ Cell Tumors	6	3	0	6	0	6	6	0
Neuronal And Mixed glioneuronal Tumors	24	4	24	0	3	21	6	18
DNT	3		3	0	0	3	0	3
Ganglioglioma	12		12	0	3	9	3	9
Central Neurocytoma	3		3	0	0	3	3	0
NOS	6		6	0	0	6	0	6
Pineal Region Tumors	2	5	0	2	0	2	2	0
Embryonal Tumors	10	6	0	10	7	3	6	4
Medulloblastoma	7		0	7	7	0	6	1
ETMR	2		0	2	0	2	0	2
Neuroblastoma	1		0	1	0	1	0	1
Total of Patients	96	–	57	39	51	45	55	41

processing software of the MR system. The susceptibility effects were identified as foci of hypointensity in the tumor on the magnitude images, and the semi-quantitative analysis method proposed by Park et al. was applied [10]. Foci of calcium, which appeared bright in phase images generated by our "right-handed" system, were subtracted from the total number of ITSS and, when acquired with greater burden, by evaluating pre-operative computed tomography images. Then, in our work the term ITSS referred only to the hemorrhagic and hypervascularization components of tumors, and was defined as low signal intensity observed within the tumor on magnitude images of SWI, including both linear and dot-like hypointense images.

The score, as validated for glioma lesions in adults, was then applied as follows: 0 = absence of ITTS, 1 = presence of 1–10 ITSS, 2 = presence of ≥ 11 ITSS [9, 11, 12] (Fig. 1).

We assessed the degree of consensus regarding ITSS score assignment; when the two radiologists initially assigned different scores to a case, the final score was achieved by consensus.

Statistical analysis

Inter-reader agreement was assessed using Cohen's κ test. We investigated how the ITSS score was correlated with histopathological grading (high grade vs. low grade) and tumor histotype (seven groups, Astrocytomas, Ependymomas, Choroid Plexuses Tumors, Germ Cell Tumors, Neuronal And Mixed glioneuronal tumors, Pineal Region Tumors, and Embryonal Tumors, and two subgroups – Astrocytomas and non astrocytomas). We also tested further subdivisions of groups based on location (supratentorial vs. infratentorial, and midline vs. off-midline).

Results

In eight cases (6 GCT, one Pineal Gland and one mixed neuronal mixed neuronal-glial tumor), calcifications were subtracted from the total calculation of the number of ITSS, using phase images and/or CT studies. For all ITSS scores, the inter-observer agreement, determined by Cohen κ, was 0.844. The agreement was 0.953 between the first reader and the consensus, and 0.890 between the second reader and the consensus.

Among all tumors, the ITSS score distribution was similar among the different locations, comparing the supratentorial versus infratentorial tumors ($p = 0.685$), and the midline versus off-midline tumors ($p = 0.124$). Although not significant, a

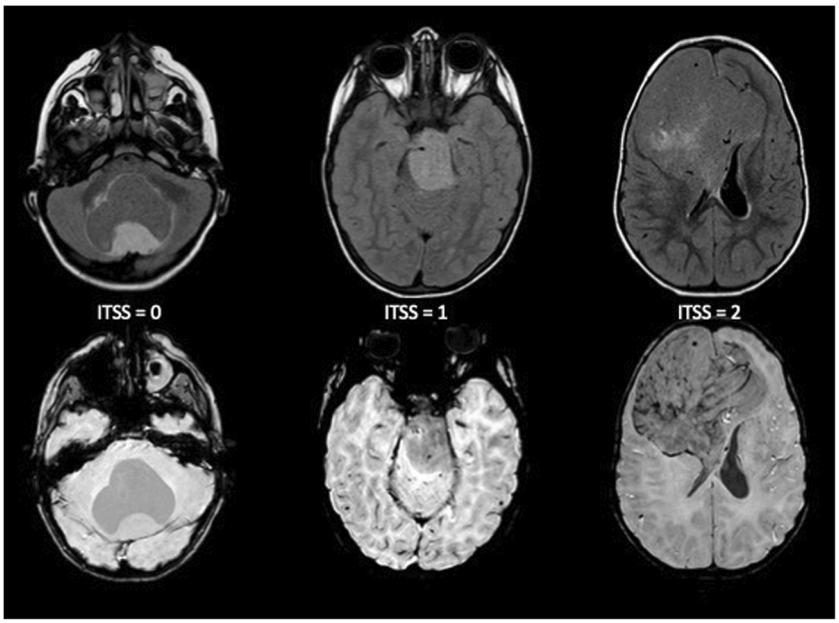

Fig. 1 Example of assignment of the ITSS score. In the upper row FLAIR images of lesions with ITSS score of 0, 1, and 2 and in the lower row the corresponding SWI images of the same masses. On the left, a pilocytic astrocytoma of the posterior cranial fossa, devoid of hypointense spots in SWI images: ITSS = 0. In the center, a H3k27m midline glioma, with only one hypointense dot: ITSS = 1. On the right a primitive encephalic neuroblastoma, with a lot of SWI hypointensities: ITSS score = 2

greater proportion of ITSS score 2 was noted in midline tumors (23/32).

In the overall population, an ITTS score of 0 correlated with low-grade tumors, and an ITTS score of 2 with high-grade tumors ($p = 0.002$). We also observed a trend of decreasing ITTS score in low-grade tumors (score 0, 25/57; score 1, 21/57; score 2, 11/57), and of increasing ITSS score in high-grade tumors (score 0, 9/39; score 1, 9/39; score 2, 21/39) (Fig. 2).

Among astrocytomas alone, we still observed a trend of lower ITTS score associated with low grade, and higher score with high grade, but with lower statistical significance ($p = 0.245$). Analysis of supratentorial astrocytomas yielded increased statistical significance ($p = 0.027$) for the correlations between a score of 0 with low grade and a score of 2 with high grade, and the distribution of scores between low-grade and high-grade tumors was similar to that among all astrocytomas. Among infratentorial astrocytomas, both low- and high-grade tumors showed a greater association with a score of 0, and a poor association with a score of 2 ($p = 0.518$). Analysis of midline astrocytomas revealed a similar distribution of ITTS scores, identifying a major association with a score of 0, and poor association with a score of 2, regardless of grade ($p = 0.356$). On the other hand, among off-midline astrocytomas, a score of 0 was associated only with low grade, and a score of 2 with high grade ($p = 0.05$).

Regarding histotype, we found that some subgroups were significantly correlated with ITSS score ($p = 0.001$). A score of 0 was associated with astrocytic tumors (23/96), whereas a score of 2 was associated with embryonal (6/96), choroid plexus (3/96), germ-cell (5/96), pineal (2/96), and ependymoma (4/96) tumors (Fig. 3). Comparing astrocytomas with all the other tumor categories revealed significant correlations between a score of 0 and astrocytomas, and between a score of 2 and non-astrocytoma tumors ($p = 0.006$), and even stronger correlations in midline location between a score of 0 astrocytomas, and between a score of 2 and non-astrocytoma tumors ($p < 0.001$) (Table 2). Considering the three most frequent pediatric tumors of the posterior cranial fossa (pilocytic astrocytoma, medulloblastoma, and ependymoma)—no medulloblastomas showed a score of 0, and 4/6 had scores of 2; PA was more frequently grade 0 (5/10) or 1 (4/10); and the four ependymomas had scores of 0 (1/4) and 2 (3/4).

Discussion

Despite only recently developed, SWI is increasingly being included in the MRI protocol for adult brain tumors, as a valuable tool for glioma grading and differentiating some tumor histotypes [8]. To our knowledge, the present study is the first to explore the use of SWI to differentiate pediatric brain tumors based on grade, type, and location. Our results support the diagnostic value of SWI for pediatric brain tumors, both in terms of tumor grading and histotype differentiation. Notably, an ITSS score of 0 usually indicated a low-grade tumor, and a score of 2 commonly indicated a high-grade tumor. However, our results are not completely superimposable with those findings regarding glioma grading among adults, which have demonstrated a significantly higher ITSS score in high-grade gliomas than in low-grade gliomas, or even the absence of ITSS in low-grade gliomas, while in our pediatric population several low grade tumors (also WHO grade I) showed ITSS score 1 and even 2 [13–15].

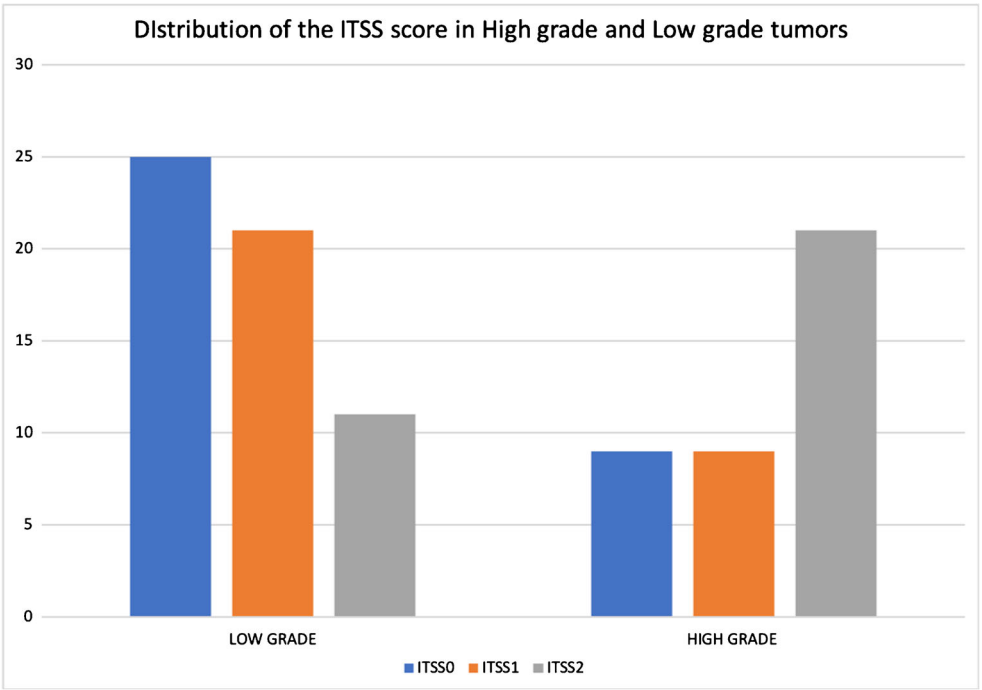

Fig. 2 Distribution of the ITSS score in high-grade and low-grade tumors

Among astrocytomas, we found a weaker correlation between ITTS score and grading, including within the subcategories (supratentorial vs. infratentorial, and midline vs. off-midline). This was likely due in part to the lack of an objective method for SWI evaluation, that could define univocally how to perform the morphologic classification, the quantification of the degree, the use of accessory sequences to be integrated in the SWI evaluation. Based on our experience, we recommend examining SWI alongside morphological MR images to ensure inclusion of the entire lesion in the ITSS score evaluation, and to avoid pitfalls due to artifacts caused by air–tissue interfaces and normal brain vessels [16]. We also assessed all corrected-phase images in comparison with magnitude images, to identify and avoid counting calcifications, and to thus optimize the ITSS score. When available, CT images were also examined. These careful evaluation methods were useful in eight cases, in which intratumoral calcifications were identified. Using this method for SWI assessment enabled easy ITSS score definition, even by less experienced physicians, showing an excellent interobserver agreement

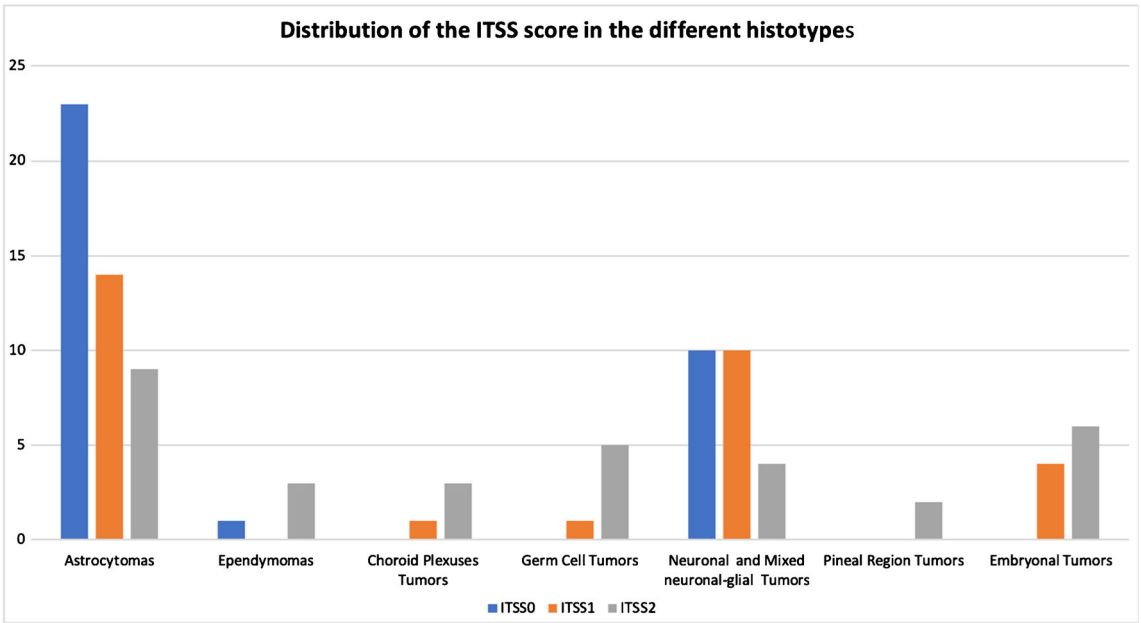

Fig. 3 Distribution of the ITSS score in the different histotypes

Table 2 Summary table of the statistical result of the ITSS correlation with location (supratentorial VS infratentorial, midline VS off-midline), histopathological classification and histotype in different subcategories

ITSS Correlation	*Tumor Subcategory*	*Results*
ITSS VS LOCATION	All	No (p = 0,685)
ITSS VS MIDLINE	All	No (p = 0,124)
ITSS VS GRADING	All	Yes (p = 0,002)
	Astrocytomas	No (p = 0,245)
	Astrocytomas – Supratentorial	Yes (*p* = 0,027)
	Astrocytomas – Infratentorial	No (p = 0,518)
	Astrocytomas – Midline	No (p = 0,356)
	Astrocytomas – Off-midline	Yes (p = 0,050)
ITSS VS HISTOTYPE	All	Yes (p = 0,001)
	Astrocytomas VS Non Astrocytomas	Yes (p = 0,006)
	Astrocytomas VS Non Astrocytomas – Midline	Yes (p < 0,001)

between a young radiology resident and an expert neuroradiologist.

The discrepancy between ITSS performance in grading adult versus pediatric astrocytomas may also be partly due to the histological peculiarity of two astrocytomas: pilocytic astrocytomas (PA) and midline gliomas H3K27m. These tumors are substantially more frequent in pediatric patients than in adults, which may promote greater variability in the distribution of ITTS scores. Although PA is a low-grade tumor (grade I), in our population, fewer than half of PA cases had an ITSS score of 0, and four reached a score of 2. These high ITSS scores in low-grade tumors were likely because PAs show abundant vascularity (described as "glomeruloid vessels") and tend to bleed due to the extensive presence of tight junctions [17]. Notably, PAs share some vascular and angiogenic features with glioblastomas [18], and glioblastomas are consistently associated with the highest ITSS score [9, 11].

On the other hand, the correct prediction of tumor grade of midline diffuse gliomas, is not feasible based on ITTS score because diffuse midline gliomas correspond to grade IV according to revised WHO 2016 classification, regardless of presence or absence of anaplastic features (like necrosis or vascular proliferation) [19, 20], if the H3K27M mutation is present. In our population, and as reported by Aboian et al., H3K27M-mutant diffuse midline gliomas showed heterogeneous histologic features in terms of vascularity and bleeding tendency, mirroring the heterogeneous appearance on MRI and SWI. Such high-grade tumors commonly had an ITSS score of 0, as low-grade astrocytomas, whereas in only two cases a score of 2 [21]. Beyond these histological differences, it also must be considered that pediatric and adult astrocytomas have different molecular profiles [22].

The concept that glioma degree increases with increasing ITSS number does not appear to be applicable in pediatric astrocytomas. One limit of the present study was that we evaluated low signal intensity in SWI based on both vasculature and hemorrhage data. While neoangiogenesis is directly associated with tumor grade, hemorrhage may not directly correlate with the extent of angiogenesis. A better method for ITSS assessment—which includes separation of hemorrhage from vasculature components [23], and combining SWI with perfusion imaging studies [6]—may allow better comprehension of the potential role of SWI in pediatric gliomas.

ITSS score was also not correlated with tumor grading within the category of mixed glioneuronal tumors, which were the second most common tumors in our cohort, after astrocytomas. All mixed glioneuronal tumors were low-grade, but ITSS scores of 0 and 1 were equally distributed, and a score of 2 was assigned in 4/24 cases. Notably, the umbrella term "mixed neuronal-glial" includes a large number of entities that present with a variety of MRI features, and variations in intratumoral bleeding. As expected, all dysembryoplastic neuroepithelial tumors presented an ITSS score of 0. In these cases, the low score was well correlated with the benign behavior of these grade I tumors, which are frequently characterized by cortical dysplasia, vascularity, and uncommon bleeding [24]. In only one case, SWI revealed a few dot-like structures, but these areas appeared "bright" on the corresponding phase images and were thus likely diamagnetic substances, such as calcification, a feature that may be present in about one-third of DNET. Thus, our experience indicates that SWI can be helpful in DNET assessment, with the use of magnitude images to exclude hemorrhage and hypervascularity, and phase images to identify calcifications.

We found low ITSS scores (0 and 1) for gangliogliomas (grade I) and NOS mixed glioneuronal tumors (grade I and II), reflecting the low aggressive behavior of these well-differentiated tumors with a slow growth pattern [25]. ITSS score showed very high performance for embryonal, pineal, and CCT tumors—with none having an ITSS score of 0, and most having a score of 2 due to the high level of intratumoral bleedings and high vascularity. The ITSS score also showed very high performance for GCT, embryonal, and pineal

tumors (all grade IV)—with none showing a score of 0, and most having a score of 2. This was likely due mainly to the high degree of intratumoral bleeding and conglomeration, rather than to high vascularity.

Central neurocytoma is a grade II tumor with a bubbly appearance and variable vascularity, which may calcify and show intratumoral hemorrhage. All central neurocytomas in our study presented a high ITSS score of 2, even after subtraction of blooming foci on SWI that corresponded to calcification on phase images. In these tumors, most of the dot-like black foci on SWI did not seem to correspond to vascular structures on 3D T1 images after gadolinium, likely reflecting the microhemorrhage etiology [26].

All ependymomas in our study were grade III, and all but one had a high ITTS score. Recent reports describe a high perfusion value [27] in terms of relative cerebral blood volume, and this very high vascularization is a likely cause of the hypointense foci on SWI. Notably, the sample for this tumor category was very small. Thus, we can only report that there was an ITSS score of 0 in a single grade III ependymoma, and cannot put forward an explanatory hypothesis.

ITSS score seemed to be randomly distributed among choroid plexus tumors, with a score of 2 assigned to two papillomas and one carcinoma. Both tumors derive from choroid plexus epithelium, appear as a hypervascular mass with frequent arteriovenous shunting, and may exhibit intralesional blood products and calcification. In a tumor category that already exhibits hypervascularization and internal bleeding in the low-grade setting, it seemed that SWI could not detect the signs of malignancy that characterized high-grade choroid plexus carcinomas—e.g., frequent mitoses, nuclear pleomorphism, increased cellular density, and necrosis invasion [28].

Our results showed a statistically significant correlation between ITTS score and specific histotypes. ITSS score was significantly lower in cases of astrocytic lesions compared to in cases of embryonal, pineal, and germ cell tumors—likely due to the poor neo-vascularization and non-bleeding tendency of the former lesions, and the high tendency towards bleeding and greater neo-vascular network of the latter.

ITSS score has proven useful for differentiating solitary enhancing brain lesions, such as GBM, metastasis, lymphomas, and nontumorous lesions [29]. More recent studies demonstrate that SWI is also useful for discriminating GBM from PCNSL in adults, and report the high sensitivity and specificity of ITSS score [8].However, after these first promising results, some later reports of hemorrhagic PCNSL (often T cell lymphomas) suggest that discrimination between PCNSL and GBM based only on ITSS may be more difficult than expected. Multiparametric analysis, including perfusion, DWI, and SWI, has been advocated to improve the diagnostic accuracy [30, 31].

SWI may also be helpful in differentiating some categories of pediatric tumors, particularly when comparing specific categories or when using a location-based approach. For instance, Morana et al. recently focused on intracranial germ cell tumors and the potential use of SWI to discriminate between midline germinomas and non-germinomatous germ cell tumors. They reported a significant difference between non-germinomatous tumors, which all showed intratumoral SWI or GRE hypointense foci, versus most of the pure germinomas, which did not [12]. Despite our low number of midline GCT cases, we found similar results, confirming that all non-germinomatous tumors had ITSS scores of 2, while we detected only two dot-like hypointensities in one pure germinoma.

With regard to the supratentorial off-midline tumors in our population, ITSS was somewhat useful for differentiating hemispheric astrocytomas from mixed glioneuronal tumors. ITSS was typically absent from neuronal and mixed glioneuronal tumors, whereas astrocytomas showed high ITSS scores.

When applying ITTS score in posterior fossa tumors, we focused on the three most frequent pediatric tumors: pilocytic astrocytoma, medulloblastoma, and ependymoma. Although our small sample did not allow statistical analysis, the results were interesting. No medulloblastoma showed a score of 0 and 4/6 had a score of 2. PAs more frequently had scores of 0 (5/10) and 1 (4/10). Among the three ependymomas, one had a score of 0 and two had a score of 2. Thus, ITTS may be useful for differentiating between medulloblastomas and pilocytic astrocytomas in the posterior fossa of children, in the sense that a score of 0 may mean that it is unlikely to be a medulloblastoma.

The present study had several limitations, some of which have already been highlighted—for example, as the method of ITSS evaluation. Assigning an ITSS score requires rigor in SWI assessment, as well as examination of the corresponding morphological images to avoid inclusion of cysts, necrosis, and normal vessels, and ensure inclusion of the whole lesion in the evaluation. Our present method yielded excellent inter-reader agreement between the radiology resident and experienced neuroradiologist. However, the methodology is not standardized in the literature, which can lead to variable reading results. We used a 1.5 T scanner with a TE of 50 ms, which involved longer acquisition times and less SNR compared to acquisitions made using 3 T scanners. However our study pointed out that a 1.5 T-systems, which is the most common machine routinely used in hospitals, can ensure good quality of SWI also in pediatric population. Finally, the main limitation was that our cohort included a relatively small sample of subjects, such that it was not possible to perform statistical analysis of all the data. Future larger studies are needed to better explore the limits and potential of SWI in pediatric brain tumors, and the possible combination of SWI with data derived from perfusion and DWI.

Conclusions

Our present results indicate that SWI, with the ITTS score, may be useful for pediatric brain tumor grading and diagnosis. The absence of ITSS was often correlated with low grade. On the other hand, the presence of ITSS, in variable numbers, was not always indicative of high grade due to the extreme histological heterogeneity of pediatric childhood tumors. Thus, ITSS score is a less reliable diagnostic tool for pediatric tumor grading than for adult glioma grading. Notably, for some groups of pediatric tumors, ITSS score may be useful for differentiating between astrocytomas and non-astrocytomas, and between pilocytic astrocytomas and medulloblastomas.

Funding information No funding was received for this study.

Compliance with ethical standards

Conflict of interest The authors declare that they have no conflict of interest.

Ethical approval All procedures performed in the studies involving human participants were in accordance with the ethical standards of the institutional and/or national research committee and with the 1964 Helsinki Declaration and its later amendments or comparable ethical standards.

Informed consent Informed consent was obtained from all individual participants included in the study.

References

1. Segal D, Karajannis MA (2016) Pediatric brain tumors: an update. Curr Probl Pediatr Adolesc Health Care 46:242–250
2. Klonou A, Piperi C, Gargalionis AN, Papavassiliou AG (2017) Molecular basis of pediatric brain tumors. NeuroMolecular Med 19:256–270
3. Saunders DE, Thompson C, Gunny R, Jones R, Cox T, Chong WK (2007) Magnetic resonance imaging protocols for paediatric neuroradiology. Pediatr Radiol 37:789–797
4. Reichenbach JR, Venkatesan R, Haacke EM et al (1997) Small vessels in the human brain: MR venography with deoxyhemoglobin as an intrinsic contrast agent. Radiology. 272-7
5. Haacke EM, Xu Y, Cheng YC, Reichenbach JR (2004) Susceptibility weighted imaging (SWI). Magn Reson Med 52: 612–618
6. Haacke EM, Mittal S, Wu Z, Neelavalli J, Cheng YC (2009) Susceptibility-weighted imaging: technical aspects and clinical applications, part 1. AJNR Am J Neuroradiol 30:19–30
7. Mittal S, Wu Z, Neelavalli J, Haacke EM (2009) Susceptibility-weighted imaging: technical aspects and clinical applications, part 2. AJNR Am J Neuroradiol 30:232–252
8. Radbruch A, Wiestler B, Kramp L, Lutz K, Bäumer P, Weiler M, Roethke M, Sahm F, Schlemmer HP, Wick W, Heiland S, Bendszus M (2013) Differentiation of glioblastoma and primary CNS lymphomas using susceptibility weighted imaging. Eur J Radiol 82: 552–556
9. Hsu CC-T, Watkins TW, Kwan GNC, Haacke EM (2016) Susceptibility-weighted imaging of Glioma: update on current imaging status and future directions. J Neuroimaging 26:383–390
10. Park MJ, Kim HS, Jahng G-H et al (2009) Semiquantitative assessment of Intratumoral susceptibility signals using non-contrast-enhanced high-field high-resolution susceptibility-weighted imaging in patients with Gliomas: comparison with MR perfusion imaging. Am J Neuroradiol 30:1402–1408
11. Saini J, Gupta PK, Sahoo P, Singh A, Patir R, Ahlawat S, Beniwal M, Thennarasu K, Santosh V, Gupta RK (2018) Differentiation of grade II/III and grade IV glioma by combining "T1 contrast-enhanced brain perfusion imaging" and susceptibility-weighted quantitative imaging. Neuroradiology 60:43–50
12. Morana G, Alves CA, Tortora D et al (2018) T2*-based MR imaging (gradient echo or susceptibility-weighted imaging) in midline and off-midline intracranial germ cell tumors: a pilot study. Neuroradiology 60:89–99
13. Xu J, Xu H, Zhang W, Zheng J (2018) Contribution of susceptibility- and diffusion-weighted magnetic resonance imaging for grading gliomas. Exp Ther Med 15:5113–5118
14. Hori M, Mori H, Aoki S, Abe O, Masumoto T, Kunimatsu S, Ohtomo K, Kabasawa H, Shiraga N, Araki T (2010) Three-dimensional susceptibility-weighted imaging at 3 T using various image analysis methods in the estimation of grading intracranial gliomas. Magn Reson Imaging 28(4):594–598
15. Aydin O, Buyukkaya R, Hakyemez B (2017) Susceptibility imaging in glial tumor grading; using 3 tesla magnetic resonance (MR) system and 32 channel head coil. Pol J Radiol 82:179–187
16. Gasparotti R, Pinelli L, Liserre R (2011) New MR sequences in daily practice: susceptibility weighted imaging. A pictorial essay. Insights Imaging 2:335–347
17. Gaudino S, Martucci M, Russo R et al (2017) MR imaging of brain pilocytic astrocytoma: beyond the stereotype of benign astrocytoma. Childs Nerv Syst 33:35–54
18. Sie M, de Bont ESJM, Scherpen FJG, Hoving EW, den Dunnen W (2010) Tumour vasculature and angiogenic profile of paediatric pilocytic astrocytoma; is it much different from glioblastoma? Neuropathol Appl Neurobiol 36:636–647
19. Khuong-Quang D-A, Buczkowicz P, Rakopoulos P, Liu XY, Fontebasso AM, Bouffet E, Bartels U, Albrecht S, Schwartzentruber J, Letourneau L, Bourgey M, Bourque G, Montpetit A, Bourret G, Lepage P, Fleming A, Lichter P, Kool M, von Deimling A, Sturm D, Korshunov A, Faury D, Jones DT, Majewski J, Pfister SM, Jabado N, Hawkins C (2012) K27M mutation in histone H3.3 defines clinically and biologically distinct subgroups of pediatric diffuse intrinsic pontine gliomas. Acta Neuropathol 124:439–447
20. Lu VM, Alvi MA, McDonald KL, Daniels DJ (2018) Impact of the H3K27M mutation on survival in pediatric high-grade glioma: a systematic review and meta-analysis. J Neurosurg Pediatr 23:308–316
21. Aboian MS, Solomon DA, Felton E, Mabray MC, Villanueva-Meyer JE, Mueller S, Cha S (2017) Imaging characteristics of pediatric diffuse midline Gliomas with histone H3 K27M mutation. AJNR Am J Neuroradiol 38:795–800
22. Georgakis MK, Tsivgoulis G, Pourtsidis A, Petridou ET (2019) Gliomatosis Cerebri among children and adolescents: an individual-patient data meta-analysis of 182 patients. J Child Neurol 34:394–401
23. Bhattacharjee R, Gupta RK, Patir R et al (2019) Quantitative vs. semiquantitative assessment of intratumoral susceptibility signals in patients with different grades of glioma. J Magn Reson Imaging. https://doi.org/10.1002/jmri.26786
24. Fernandez C, Girard N, Paredes AP (2003) The usefulness of MR imaging in the diagnosis of dysembryoplastic neuroepithelial tumor

in children: a study of 14 cases. AJNR Am J Neuroradiol 24(5): 829–834
25. She D-J, Lu Y-P, Xiong J et al (2019) Comparison of conventional, diffusion, and perfusion MRI between infratentorial ganglioglioma and pilocytic astrocytoma. Acta Radiol 60:1687–1694
26. Zhang B, Luo B, Wen J et al (2004) Central neurocytoma: a clinicopathological and neuroradiological study. Neuroradiology. 46(11):888–895
27. Gupta PK, Saini J, Sahoo P et al (2017) Role of dynamic contrast-enhanced perfusion magnetic resonance imaging in grading of pediatric brain tumors on 3T. Pediatr Neurosurg 52:298–305
28. Lin H, Leng X, Qin C-H et al (2019) Choroid plexus tumours on MRI: similarities and distinctions in different grades. Cancer Imaging 19:17
29. Kim HS, Jahng G-H, Ryu CW, Kim SY (2009) Added value and diagnostic performance of intratumoral susceptibility signals in the differential diagnosis of solitary enhancing brain lesions: preliminary study. AJNR Am J Neuroradiol 30:1574–1579
30. Saini J, Kumar Gupta P, Awasthi A et al (2018) Multiparametric imaging-based differentiation of lymphoma and glioblastoma: using T1-perfusion, diffusion, and susceptibility-weighted MRI. Clin Radiol 73:986.e7–986.e15
31. Kim EY, Kim SS (2005) Magnetic resonance findings of primary central nervous system T-cell lymphoma in Immunocompetent patients. Acta Radiol 46:187–192

Affiliations

Simona Gaudino[1] · Giammaria Marziali[1,2] · Giovanna Pezzullo[3] · Pamela Guadalupi[1,2] · Carolina Giordano[1,2] · Amato Infante[4] · Massimo Benenati[1,2] · Antonia Ramaglia[1,2] · Luca Massimi[5,6] · Marco Gessi[7] · Paolo Frassanito[5] · Massimo Caldarelli[5,6] · Cesare Colosimo[1,2]

1 UOC Radiodiagnostica e Neuroradiologia, Dipartimento di Diagnostica per Immagini, Radioterapia, Oncologia ed Ematologia, Fondazione Policlinico Universitario A. Gemelli IRCCS, Rome, Italy

2 Istituto di Radiologia, Università Cattolica del Sacro Cuore, Rome, Italy

3 Dipartimento di Scienze Biomediche Avanzate, Università degli Studi di Napoli "Federico II", Naples, Italy

4 Dipartimento di diagnostica per immagini, Radioterapia Oncologica e Ematologia, Fondazione Policlinico Universitario A. Gemelli IRCCS, Rome, Italy

5 Pediatric Neurosurgery, Neurosurgery Department, Fondazione Policlinico Universitario A. Gemelli IRCCS, Rome, Italy

6 Istituto di Neurochirurgia, Università Cattolica del Sacro Cuore, Rome, Italy

7 Neuropathology Unit, Division Of Pathology, Fondazione Policlinico Universitario A. Gemelli, Università Cattolica del Sacro Cuore, Rome, Italy